Communication between L-galactono-1,4-lactone dehydrogenase and cytochrome c

Journal:	*FEBS Journal*
Manuscript ID:	FJ-12-0955.R1
Manuscript Type:	Regular Paper
Subdiscipline:	Enzymes and catalysis
Date Submitted by the Author:	08-Feb-2013
Complete List of Authors:	Hervás Morón, Manuel; University of Seville, Dept. of Biochemistry Bashir, Qamar; Leiden University, Gorlaeus Labs., Leiden Institute of Chemistry Leferink, Nicole; University of Manchester, Manchester Interdisciplinary Biocentre Ferreira Neila, Patricia; University of Zaragoza, Dept. of Biochemistry & Molecular & Cellular Biology Moreno-Beltrán, Blas; University of Seville, CSIC, Inst. of Plant Biochemistry & Photosynthesis Westphal, Adrie; Wageningen University, Laboratory of Biochemistry Díaz-Moreno, Irene; University of Seville, CSIC, Inst. of Plant Biochemistry & Photosynthesis Medina Trullenque, María Milagros; University of Zaragoza, Dept. of Biochemistry & Molecular & Cellular Biology De la Rosa Acosta, Miguel; University of Sevilla CSIC, Inst. of Plant Biochemistry & Photosynthesis Ubbink, Marcellus; Leiden University, Gorlaeus Labs., Leiden Inst. of Chemistry Navarro Carruesco, José; University of Seville, Biochemistry van Berkel, Willem; Wageningen University, Lab. of Biochemistry
Key Words:	cytochrome c, electron transfer, flavoprotein, protein-protein interaction, vitamin C

FEBS Journal

Communication between L-galactono-1,4-lactone dehydrogenase and cytochrome *c*

Manuel Hervás[1], *Qamar Bashir*[2,5], *Nicole G. H. Leferink*[3,6], *Patricia Ferreira*[4], *Blas Moreno-Beltrán*[1], *Adrie H. Westphal*[3], *Irene Díaz-Moreno*[1], *Milagros Medina*[4], *Miguel A. de la Rosa*[1], *Marcellus Ubbink*[2], *José A. Navarro*[1] & *Willem J. H. van Berkel*[3]

[1] Instituto de Bioquímica Vegetal y Fotosíntesis, CSIC and University of Sevilla, cicCartuja, Américo Vespucio 49, 41092-Seville, Spain.

[2] Gorlaeus Laboratories, Leiden Institute of Chemistry, Leiden University, Einsteinweg 55, 2333 CC Leiden, The Netherlands

[3] Laboratory of Biochemistry, Wageningen University, Dreijenlaan 3, 6703 HA Wageningen, The Netherlands

[4] Department of Biochemistry and Molecular and Cell Biology and Institute for Biocomputation and Physics of Complex Systems, University of Zaragoza, C/Pedro Cerbuna 12, 50009 Zaragoza, Spain

[5] Present address: School of Biological Sciences, University of the Punjab, Quaid-e-Azam Campus, Lahore 54590, Pakistan

[6] Present address: Manchester Interdisciplinary Biocentre and Faculty of Life Sciences, University of Manchester, Manchester M1 7DN, United Kingdom

Running title: Interaction between mitochondrial redox proteins

Corresponding author. W. J. H. van Berkel, Laboratory of Biochemistry, Wageningen University, Dreijenlaan 3, 6703 HA Wageningen, The Netherlands. E-mail: willem.vanberkel@wur.nl; phone +31-317-482861; fax: +31-317-484801

FEBS Journal

Abbreviations. Cc_{OX}, Cc_{RED}, cytochrome c, Cc, in its oxidized or reduced form. $GALDH_{OX}$, $GALDH_{SQ}$, $GALDH_{HQ}$, L-galactono-1,4-lactone dehydrogenase, GALDH, in its oxidized, semiquinone or hydroquinone forms; ΔH, ΔS, binding enthalpy and entropy values, respectively, for the GALDH:Cc interaction; k_{obs}, observed pseudo-first-order rate constant; K_A, association constant; K_D, dissociation constant; k_{ET}, first-order rate constant for intracomplex electron transfer; k_2, second-order rate constant for bimolecular electron transfer; k_{inf}, second-order rate constant extrapolated to infinite ionic strength; ITC, isothermal titration calorimetry; PDQ, propylene-diquat; n, GALDH:Cc binding stoichiometry; NMR, nuclear magnetic resonance; dRf, $dRfH^{\cdot}$, 5-deazariboflavin and its reduced radical.

Enzymes. L-galactono-1,4-lactone dehydrogenase (L-galactono-1,4-lactone: ferricytochrome c oxidoreductase, EC 1.3.2.3)

Keywords. cytochrome *c*, electron transfer, flavoprotein, protein-protein interaction, vitamin C

Subdivision. Enzymes and catalysis

FEBS Journal

SUMMARY

L-galactono-1,4-lactone dehydrogenase (GALDH) catalyzes the terminal step of vitamin C biosynthesis in plant mitochondria. Here we investigated the communication between *Arabidopsis thaliana* GALDH and its natural electron acceptor cytochrome *c* (Cc). Using laser-generated radicals we observed formation and stabilization of the GALDH semiquinone anionic species ($GALDH_{SQ}$). $GALDH_{SQ}$ oxidation by Cc exhibited a non-linear dependence on Cc concentration consistent with a kinetic mechanism involving protein-partner association to form a transient bimolecular complex prior to the electron transfer step. Oxidation of $GALDH_{SQ}$ by Cc was significantly impaired at high ionic strength, revealing the existence of attractive charge-charge interactions between both reactants. Isothermal titration calorimetry showed that GALDH weakly interacts with both oxidized and reduced Cc. Chemical shift perturbations for ^{1}H and ^{15}N nuclei of Cc, arising from the interactions with unlabelled GALDH, were used to map the interacting surface of Cc. For *Arabidopsis* Cc and yeast Cc, similar residues are involved in the interaction with GALDH. These residues are confined to a single surface surrounding the heme edge. The range of chemical shift perturbations for the physiological *Arabidopsis* Cc-GALDH complex is larger than that of the non-physiological yeast Cc-GALDH complex, indicating that the former complex is more specific. In summary, the results point to a relatively low-affinity GALDH/Cc interaction, similar for all partner redox states, involving protein-protein dynamic motions. Evidence is also provided that Cc utilizes a conserved surface surrounding the heme edge for the interaction with GALDH and other redox partners.

***Database*:** NMR assignment of the backbone amide resonances of *Arabidopsis* Cc_{RED} has been deposited in BMRB database (**BMRB accession number 18828**).

INTRODUCTION

Flavoenzymes are ubiquitous in nature, taking part in a large variety of biochemical reactions [1]. Flavoprotein dehydrogenases, in particular, oxidize a wide range of organic substrates and mainly use quinones and electron transfer proteins as electron acceptors [2].

L-galactono-1,4-lactone dehydrogenase (GALDH; EC 1.3.2.3) is a FAD-containing oxidoreductase that catalyzes the terminal step of the Smirnoff-Wheeler pathway of vitamin C (L-ascorbate) biosynthesis in plants [3, 4]. The mitochondrial enzyme uses cytochrome c (Cc) as electron acceptor. GALDH homologs in animals (L-gulono-1,4-lactone oxidase), yeast (D-arabinono-1,4-lactone oxidase), and fungi (D-gluconolactone oxidase) use molecular oxygen as electron acceptor and are involved in the synthesis of L-ascorbate or its analogs D-erythorbate and D-erythroascorbate [3, 5]. Evidence is accumulating that GALDH, next to its paramount enzymatic function, is essential for assembly of the respiratory NADH dehydrogenase complex (complex I) [6].

The catalytic cycle of GALDH consists of the acceptance of two electrons from the carbohydrate to reduce the flavin cofactor (reductive half-reaction) and the transfer of these electrons to two Cc molecules (oxidative half-reaction). Re-oxidation of the two-electron reduced enzyme ($GALDH_{HQ}$) by Cc occurs in two single-electron steps and involves the intermediate formation of the anionic flavin semiquinone ($GALDH_{SQ}$) [3]. Here we performed a kinetic and thermodynamic study of the GALDH/Cc interaction and electron-transfer reactions, by using laser-flash photolysis and stopped-flow kinetic analysis as well as isothermal titration calorimetry and NMR spectroscopy. The results point to a transient, highly dynamic GALDH/Cc interaction, similar for all partner redox states. Evidence is also provided that Cc employs a conserved surface for interaction with its multiple partners.

RESULTS

Laser-flash spectroscopy – By using laser-flash spectroscopy and flavins as redox probes, it is possible to induce one-electron reductions and follow fast electron transfer processes in redox proteins [7]. GALDH reduction, either by laser-generated deazariboflavin ($dRfH^{\cdot}$) or propylene diquat ($PDQ^{\cdot+}$) radicals, results in decrease in absorbance of the flavin cofactor in the 400-500 nm range, without significant increase at longer wavelengths (not shown). This is consistent with the very rapid formation of the $GALDH_{SQ}$ anionic species [3, 8], which is stable in a time-scale of hundreds of milliseconds (Figure 1, traces A-B). From the kinetic traces shown in Figure 1, it is possible to calculate the observed pseudo-first-order rate constant (k_{obs}) for $GALDH_{SQ}$ formation. From the slope of the linear plot of k_{obs} *versus* GALDH concentration (not shown), a k_2 of 5.5 x 10^7 $M^{-1}s^{-1}$ for GALDH reduction by $dRfH^{\cdot}$ is obtained. By using the positively-charged $PDQ^{\cdot+}$ radical it is possible to improve the one-electron reduction rate of GALDH (k_2 = 1.2 x 10^8 $M^{-1}s^{-1}$), as previously shown for other proteins with a negatively-charged active site [9, 10].

Both $dRfH^{\cdot}$ (E'_m = -650 mV) and $PDQ^{\cdot+}$ (E'_m = -550 mV) can also directly reduce Cc (k_2 = 6.2 x 10^8 $M^{-1}s^{-1}$ and 2.5 x 10^8 $M^{-1}s^{-1}$, respectively) (not shown). Although the less reductive midpoint reduction potential of Cc (E'_m = +250 mV) favors its reduction by $dRfH^{\cdot}$ or $PDQ^{\cdot+}$ as radical donor, it is possible, by using high concentrations of GALDH (ca. 50 µM) and PDQ as intermediate, to observe a preferential reduction of GALDH and only a small contribution of direct Cc reduction. To avoid interferences arising from direct Cc reduction by PDQ, the redox changes associated to GALDH were monitored at 433 nm, which is an isosbestic point for the oxidized and reduced forms of Cc (Figure 1).

When *Arabidopsis* Cc is added to a reaction cell containing GALDH, the laser-induced absorbance changes fit well with the initial fast reduction of GALDH followed by its oxidation on a longer time scale (Figure 1, trace C). The $GALDH_{SQ}$ oxidation observed at 433 nm is concomitant with the electron transfer to Cc, as inferred from the absorbance increase at 550 nm in the same time frame (not shown). The k_{obs} values for $GALDH_{SQ}$ oxidation by Cc present a non-linear dependence on Cc concentration (Figure 2, upper panel). This kind of concentration dependence has been previously explained in terms of a kinetic mechanism involving protein-partner association to form a transient electron transfer bimolecular complex prior to the electron transfer step [10-12]. Applying the formalism developed by Meyer et al [12], the minimal values for the electron transfer step rate (k_{ET}) and the

association and dissociation (K_A, K_D) constants can be estimated (Table 1). For comparative purposes, we also performed experiments with horse Cc, obtaining qualitatively similar results (Figure 2, upper panel, and Table 1).

The effect of ionic strength on the interaction of $GALDH_{SQ}$ with Cc was analyzed in order to investigate the electrostatic nature of the interaction. As can be seen in Figure 2 (lower panel), when studying the interaction between $GALDH_{SQ}$ and horse Cc, the k_{obs} values decrease monotonically with increasing salt concentration up to 150 mM NaCl (175 mM ionic strength). In addition, the k_{obs} values show linear concentration dependencies on Cc at high salt concentration, suggesting a second-order collisional process with no formation of any kinetically detectable electron transfer complex. Thus, oxidation of $GALDH_{SQ}$ by horse Cc is significantly impaired at high ionic strength, revealing the existence of attractive charge-charge interactions between both reactants. The bimolecular second-order k_2 values for the GALDH/Cc interaction at infinite ionic strength (k_{inf}) can be directly estimated (Table 1). Almost identical results are obtained with *Arabidopsis* Cc at relatively higher NaCl concentrations (≥ 20 mM; 45 mM ionic strength) (Figure 2, lower inset, and Table 1). From this set of data similar values for k_{inf} are estimated for both cytochromes, which reflects the intrinsic reactivity of the partners without considering charge-charge interactions (Table 1) [13]. More interesting, however, is the behavior observed with *Arabidopsis* Cc at low ionic strength (Figure 2, lower panel), at which a biphasic dependence of k_{obs} with NaCl concentration is observed. This bell-shaped profile reflects a rearrangement of the initial GALDH/Cc interaction complex to achieve optimal electron transfer, as previously reported for other protein systems, indicating the occurrence of protein-protein dynamic motions that are blocked by strong electrostatics at very low ionic strength [11, 14].

Stopped-flow experiments of mixing $GALDH_{HQ}$ with *Arabidopsis* Cc at low ionic strength showed that GALDH oxidation mostly occurs within the dead time of the instrument (k_{obs} > 200 s^{-1}), as demonstrated by the appearance of the reduced Cc spectrum immediately after mixing (not shown). Only when assaying at a salt concentration of 150 mM slower kinetics of GALDH oxidation, linearly dependent on Cc concentration, could be observed (Figure 2, lower inset). The estimated k_2 value of ca. 10^7 $M^{-1}s^{-1}$ (Table 1) is similar to the corresponding value for $GALDH_{SQ}$ oxidation at the same salt concentration measured by laser-flash spectroscopy (Figure 2, lower inset, and Table 1).

Isothermal titration calorimetry – The interaction between both oxidized and reduced *Arabidopsis* Cc with GALDH was studied by ITC. Figure 3 shows the calorimetric titration of $GALDH_{OX}$ by Cc_{OX}. From the dependence of the heat evolved during Cc titration it is possible to calculate a binding GALDH/Cc stoichiometry ≈ 1 for both Cc_{OX} and Cc_{RED} (Figure 3), as well as the K_A and K_D and the ΔH and –TΔS values for the binding process (Table 1). As shown in Table 1, the thermodynamic parameters are equivalent for the interaction with the two redox forms of Cc, with similar K_D values of 17 μM (K_A = 5.9 x 10^4 M^{-1}; ΔG = -27.3 kJ mol^{-1}) and 13 μM (K_A = 7.7 x 10^4 M^{-1}; ΔG = -27.9 kJ mol^{-1}) at an ionic strength of about 13 mM for Cc_{OX} and Cc_{RED}, respectively, and also similar to the estimated value for the interaction of $GALDH_{SQ}$ with Cc_{OX} measured by laser spectroscopy (Table 1). The data also indicate a binding process mainly driven by entropic factors, as deduced from the ΔH and –TΔS values (Table 1). Thus, the results indicate an enthalpic contribution opposing the binding, although strong charge-charge interactions between the partners are occurring at the low ionic strength used. Therefore, the favorable entropic contribution to binding probably indicates removal of water molecules from the protein-protein interaction area upon forming the complex, or the release of water molecules that surround the charges.

NMR binding studies - The interaction between GALDH and Cc was further addressed by titrating ^{15}N labeled Cc into unlabelled GALDH in a series of NMR experiments. For each titration point the amide peaks were recorded in the [^1H, ^{15}N] HSQC spectrum. The binding of the two proteins was evidenced by the increase in line-width of all peaks in the NMR spectrum and chemical shift changes of certain nuclei. For all titrations, a single set of amide peaks was observed in the HSQC spectra showing that the GALDH/Cc complex is in fast exchange on NMR time scale (k_{off} > 125 s^{-1}). The Cc residues involved in interaction with GALDH were identified on the basis of size of their chemical shift perturbations and the interaction surface on Cc was mapped (Figure 4 and 5). The chemical shift changes in ^{15}N dimension ($\Delta\delta^N$) were more significant than those in ^1H dimension ($\Delta\delta^H$). For the interaction of $GALDH_{OX}$ with both yeast Cc_{OX} and *Arabidopsis* Cc_{RED}, the overall size of the chemical shift perturbations was small, indicating that the complexes are transient and highly dynamic. The residues of yeast Cc showing the highest chemical shift perturbations (> 0.25 ppm for ^{15}N) are conserved in both *Arabidopsis* Cc paralogs, including Thr12 (Figure S1), suggesting

that the interaction of GALDH and its physiological electron acceptors involves a similar mechanism.

The chemical shift perturbations of several residues were plotted against Cc/GALDH ratio and the dissociation constant of the complex was estimated by fitting these curves to a 1:1 binding model (Figure 6). From the global fit of these titration curves, the K_D of the yeast Cc_{OX}-$GALDH_{OX}$ complex and *Arabidopsis* Cc_{RED}-$GALDH_{OX}$ complex were determined to be 50 μM and 77 μM, respectively (K_A values of 2.0 x 10^4 M^{-1} and 1.3 x 10^4 M^{-1}) at an ionic strength of about 50 mM.

In a number of NMR studies, the size of the chemical shift perturbations has been reported to correlate with the extent of dynamics in protein complexes [15-18]. The proteins in specific complexes have a single well-defined orientation for most of the time, resulting in large size of the chemical shift changes. In highly dynamic complexes the encounter state constitutes a considerable fraction of the complex. The encounter state consists of multiple, fast exchanging orientations. The chemical shift changes are averaged over all these orientations resulting in a small size. Furthermore, desolvation of the surface may be limited in the encounter state, as compared to the specific complex, also reducing the perturbations of the amide resonances. The complexes of GALDH with yeast Cc and *Arabidopsis* Cc exhibit a small average size of the chemical shift changes suggesting that the complexes are highly dynamic, comprising of significant fractions of the encounter complexes. The *Arabidopsis* Cc shows somewhat larger chemical shift changes upon complex formation with GALDH as compared to those for the yeast GALDH/Cc complex (Figure 4).

DISCUSSION

GALDH is an aldonolactone oxidoreductase that belongs to the vanillyl-alcohol oxidase flavoprotein family [19]. Members of this family share a characteristic two-domain folding topology formed by a conserved N-terminal FAD-binding domain and a less conserved C terminal cap-domain that determines the substrate specificity.

GALDH is localized in the mitochondrial inner membrane space where it is involved in feeding electrons into the electron transport chain [20, 21]. GALDH reacts poorly with molecular oxygen and is sensitive towards irreversible oxidation during oxidative stress [22]. This might be one of the reasons why GALDH is a dehydrogenase and not, like other aldonolactone oxidoreductases, an oxidase [23]. Here we studied the kinetic and thermodynamic interplay of GALDH with its natural electron acceptor Cc.

Using laser-flash spectroscopy we could demonstrate that GALDH reduction, either by dRfH$^{\cdot}$ or $PDQ^{\cdot+}$ radicals, results in the very rapid formation of anionic $GALDH_{SQ}$ and that this species is stable in a time-scale of hundred of milliseconds. The highest reduction rates were observed with $PDQ^{\cdot+}$ (k_2 = 1.2 x 10^8 $M^{-1}s^{-1}$), indicative for a negatively-charged protein active site.

$GALDH_{SQ}$ oxidation by *Arabidopsis* Cc at low ionic strength showed a non-linear dependence on Cc concentration, indicative for the formation of a transient protein complex prior to the electron transfer step. Somewhat faster reactions with GALDH were observed when laser-flash experiments were performed with horse Cc, as compared to the natural *Arabidopsis* Cc partner. However, quite similar values for k_{ET} and K_D were obtained, suggesting similar modes of interaction between GALDH and both cytochromes. The differences observed in the reactivity of both Cc at low ionic strength can be rationalised not only in terms of differences in the total net charge of both proteins (p*I* of ca. 10 *versus* 9.5 for horse and *Arabidopsis* Cc, respectively) but also in subtle differences arising from specific charge localisations on the surfaces of both cytochromes (Figure S1).

Very similar results were obtained when the interaction of $GALDH_{SQ}$ with both *Arabidopsis* and horse Cc was studied at high ionic strength, the data being consistent with a second-order collisional process with no electron transfer complex formation. These results not only reveal the intrinsic reactivity between the redox partners ($k_{inf} \approx 10^6$ $M^{-1}s^{-1}$), but also point to the existence of dynamic charge-charge interactions at low ionic strength. With *Arabidopsis* Cc, these charge-charge interactions might hamper dynamic motions within the

complex, as concluded from the decrease in electron transfer rate observed at very low ionic strength.

Reaction of $GALDH_{HQ}$ with *Arabidopsis* Cc is very fast. Kinetics could only be followed in the stopped-flow spectrophotometer at relatively high ionic strength, where comparable rates are obtained for both $GALDH_{SQ}$ and $GALDH_{HQ}$ oxidation by Cc. Although it is not possible to accurately compare the stopped-flow and laser-flash data at low ionic strength, taken together, and according to previously published data on the GALDH:L-galactono-1,4-lactone interaction [3], they suggest that reduction of GALDH by its carbohydrate substrate limits the overall rate of GALDH-mediated Cc reduction.

ITC experiments showed that $GALDH_{OX}$ forms a weak stoichiometric complex with both *Arabidopsis* Cc_{OX} and Cc_{RED} and that binding is mainly determined by entropic factors. The K_D values of ≈ 17 µM and 13 µM for the complexes with Cc_{OX} and Cc_{RED}, respectively, were very similar and in the same range as found for $GALDH_{SQ}$ using laser-flash kinetic analysis. The weak interaction between GALDH and Cc was confirmed by NMR experiments, yielding a K_D value of ≈ 50 µM for the yeast Cc_{OX}/$GALDH_{OX}$ complex and a K_D value of ≈ 77 µM for the *Arabidopsis* Cc_{RED}/$GALDH_{OX}$ complex. The K_D value for the *Arabidopsis* Cc_{RED}/$GALDH_{OX}$ complex is somewhat higher than the corresponding value found with ITC, probably due to the higher ionic strength of the medium for the NMR studies.

The chemical shift perturbation experiments established that yeast Cc and *Arabidopsis* Cc use similar residues surrounding the heme edge for interaction with GALDH. Interestingly, binding maps of Cc in the complexes with GALDH (this work), cytochrome b_5 [16] and the non-physiological partner adrenodoxin [18] are strikingly similar. Moreover, chemical shift mapping studies of Cc in the complexes with bovine cytochrome b_5 [16], yeast Cc peroxidase [24], cyanobacterial cytochrome *f* [25], pea plastocyanin [26], and GALDH (this work) indicate that Thr12 (Gln12 in horse Cc used in ref. [26]) shows the biggest binding shifts. This finding indicates that Cc employs a conserved set of surface-exposed residues for the interactions with a variety of proteins.

There are several buried Cc residues whose chemical shift perturbations cannot be explained by the direct interaction with a partner protein. Most likely, these are caused by transmittance of the binding effects from the surface of the protein to its core via covalent and hydrogen bonds [26]. The size of Δδ observed for the GALDH/Cc complex is small, which can be explained by multiple fast-exchanging protein-protein orientations within the complex,

for which the observed Δδ would be averaged over all orientations. This suggests that Cc and GALDH adopt different relative orientations within the complex, rather than forming a single, well defined structure [27].

The GALDH-Cc complex represents an example of a transient complex characterized by low binding affinity and millisecond lifetime. Transient complex formation occurs between proteins in situations that fast turnover of the complex is required for biological function. Electron transfer proteins are known to form very short-lived complexes. In such complexes a balance must be found between affinity (and thus specificity) and a high dissociation rate. Furthermore, usually these proteins react with more than one partner using a single surface patch, which also compromises specificity. Rapid complex formation is achieved by complementary electrostatic forces and proceeds through the formation of the encounter state. This state exists as a considerable fraction of the complex in dynamic equilibrium with the specific complex. The encounter state is thought dominated by long-range electrostatic interactions, thus limiting the specificity of the interaction in this stage of complex formation. The specific complex is formed to achieve fast electron transfer to a specific partner. In some cases the encounter complex comprises itself electron transfer active orientations and a specific complex is not formed. The very small chemical shift perturbations observed for Cc in complex with GALDH suggest that the encounter state is dominant in this case, in particular for yeast Cc, which shows overall smaller perturbations than *Arabidopsis* Cc.

In summary, we demonstrated that GALDH forms a transient low-affinity complex with Cc. The interaction involves protein-protein dynamic motions and entropic factors. In addition, the affinity of GALDH for Cc is similar for all the different redox states of both partners. This relatively non-specific interaction does not preclude rapid electron transfer within the complex, because sufficient ET permissible conformations are apparently sampled in this dynamic complex.

EXPERIMENTAL PROCEDURES

Chemicals –L-galactono-1,4-lactone, L-gulono-1,4-lactone, ß-dodecyl-maltoside, bovine Cc and horse Cc were from Sigma-Aldrich (St Louis, MO, USA). All other chemicals were from commercial sources and of the purest grade available. Deazariboflavin and propylene diquat were a generous gift from Prof. Gordon Tollin (University of Arizona, USA).

Protein purification and analysis – GALDH-His_6 was expressed and purified as reported earlier [3]. *Arabidopsis* Cc (cytochrome c-2 isoform, NCBI NP_192742) was expressed and purified as described previously [10]. Isotopically-enriched ^{15}N yeast and plant Cc were produced in *E. coli* and purified as reported previously [28, 29].

Desalting or buffer exchange of small aliquots of enzyme was performed with Bio-Gel P-6DG columns (Bio-Rad). Absorption spectra were recorded at 25 °C on a Hewlett Packard (Loveland, CO, USA) 8453 diode array spectrophotometer in 50 mM sodium phosphate, pH 7.4.

GALDH concentrations were determined using an absorption coefficient of 12.9 mM^{-1} cm^{-1} at 450 nm [3]. Cc_{OX} and Cc_{RED} stock solutions were prepared, essentially as described elsewhere [16]. Cc_{RED} concentrations were determined using absorption coefficients of 31.8 (*Arabidopsis*), 27.5 (yeast) and 30.8 (horse) mM^{-1} cm^{-1} at 550 nm [10, 30, 31].

Laser-flash spectroscopy – Laser-flash experiments were performed anaerobically at 25 °C in a 1 cm path-length cuvette using EDTA as electron donor and dRf as photosensitizer in the presence of PDQ, as previously described [9, 32, 33]. The laser flash generates $dRfH^{\cdot}$ radicals which, in the presence of an excess of PDQ, rapidly (< 1 µs) react with the viologen analogue to form its reduced species ($PDQ^{\cdot+}$) [9], that is able to reduce $GALDH_{OX}$ to form $GALDH_{SQ}$. The standard reaction mixture contained, in a final volume of 1.5 mL, 10 mM Tris-HCl buffer, pH 7.5, 2 mM EDTA, 100 µM dRf, 1 mM PDQ, 0.02% ß-dodecyl-maltoside, 50 µM $GALDH_{OX}$ and Cc_{OX} at varying concentrations. The redox changes of GALDH in GALDH/Cc mixtures were monitored at 433 nm, an isosbestic point for Cc, thus avoiding interferences arising from any direct reduction of Cc by the dRf/PDQ system. For ionic-strength dependence experiments, small amounts of a concentrated stock solution of NaCl were added to the sample. All experiments were performed under pseudo-first-order conditions, for which the amount of acceptor (Cc_{OX}) was maintained well in excess over the

amount of the generated $GALDH_{SQ}$ (< 1 µM). Each kinetic trace was the average of 6-10 measurements. Kinetic analyses were performed according to the reaction mechanisms previously proposed [12, 13] to obtain the second-order bimolecular rate constant (k_2), the association constant (K_A) and the electron-transfer rate constant (k_{et}) values [12], as well as the second-order rate constant at infinite ionic strength (k_{inf}) by fitting the ionic strength data with the theoretical model for electrostatic interactions previously described [12, 13]. Estimated errors in the determined values were ±10%.

Stopped-flow kinetics - Stopped-flow experiments were carried in 20 mM phosphate buffer, pH 7.5, at 25 ºC under anaerobic conditions using a µSFM-20 device fitted with a TC-50/10 cuvette and coupled to a MOS-450 spectrophotometer (Bio-Logic). $GALDH_{HQ}$ was generated *in situ* in the stopped-flow syringe by incubating with 1 mM L-gulono-1,4-lactone (a commercially available isomer of L-galactono-1,4-lactone) [3]. 200 µL solutions of 7 µM $GALDH_{HQ}$ were mixed with small volumes of Cc_{RED} stock solutions (≥ 100 µM), and the evolution of the process was followed at 550 nm. The observed rate constants (k_{obs}) were calculated by fitting to mono-exponential processes by using the Bio-Kine32 software package from the manufacturer. Estimated errors in the determined values were ±15%.

Isothermal calorimetry - The interaction between $GALDH_{OX}$ and *Arabidopsis* Cc_{OX} or Cc_{RED} was studied by isothermal titration calorimetry (ITC) at 25 ºC in a CSC Model 500 Nano-ITC III in 5 mM sodium phosphate, pH 7.5, supplemented with 0.01% ß-dodecyl-maltoside. 120 µM $GALDH_{OX}$ solutions were titrated with successive additions (7-10 µL) of concentrated solutions of either Cc_{OX} or Cc_{RED}. Thermodynamic parameters were calculated by data fitting using the MicroCal Origin software to obtain the binding stoichiometry (n), the K_A (and K_D) and the binding enthalpy (ΔH) and entropy (ΔS) values for the interaction process [34]. Estimated errors in the determined values were ±10%.

NMR assignments – NMR assignments of the ^{15}N and ^{1}H nuclei of yeast Cc_{OX} were taken from previous work [24] and a recent study with several corrections [35]. NMR assignment experiments of the ^{15}N and ^{1}H nuclei for *Arabidopsis* Cc_{RED} were performed on a Bruker Avance 700 MHz NMR spectrometer operating at 25 ºC. For the sequence-specific assignment of the backbone amide resonances of *Arabidopsis* Cc_{RED}, a 2D [^{1}H, ^{15}N] HSQC,

3D [^{1}H, ^{15}N] NOESY-HSQC with 100 ms mixing time and 3D [^{1}H, ^{15}N] TOCSY-HSQC spectra were recorded. The NMR sample contained 2.0 mM of uniformly ^{15}N labeled *Arabidopsis* Cc_{RED} in 5 mM sodium phosphate pH 6.0 and 10% D_2O for lock. The data were processed using Bruker TopSpin and NMRPipe [36] and further analyzed by SPARKY [T. D. Goddard and D. G. Kneller, SPARKY 3, University of California, San Francisco]. NMR assignment has been deposited in BMRB database (**BMRB accession number 18828**).

NMR titrations – NMR samples (0.5 mL) contained 70 nmoles of unlabelled GALDH and varying concentrations of ^{15}N labelled yeast Cc_{OX} or *Arabidopsis* Cc_{RED} in 20 mM sodium phosphate pH 7.4, 6% D_2O for lock, and 0.1 mM $CH_3CO^{15}NH_2$ as internal reference. The pH of the samples was checked before and after each titration step and adjusted, if necessary, with small aliquots of 0.1 M NaOH or 0.1 M HCl solutions. Titrations consisted of 13 experimental points with 0, 20, 35, 50, 75, 100, 125, 150, 175, 200, 225, 250, and 300 nmoles of the ^{15}N labeled Cc.

The chemical shift changes were monitored in a series of [^{1}H, ^{15}N] HSQC experiments at 30 ºC, recorded on a Bruker DMX600 MHz equipped with TCI-Z-GRAD cryoprobe. [^{1}H, ^{15}N] HSQC spectra were acquired with 1024 and 90 complex points in ^{1}H and ^{15}N dimensions, respectively. The data were processed in NMRPipe [36] and analysed in CcpNmr [37].

NMR chemical shift titration curves were analyzed with a two parameter non-linear least squares fit using a one site binding model, as given by the following equation:

$$\Delta\delta = \tfrac{1}{2}\Delta\delta_0\left[A - \sqrt{A^2 - \frac{4}{R}}\right] \quad (1a)$$

$$A = 1 + \tfrac{1}{R} + \frac{[Cc]_0 + R[GALDH]_0}{R[Cc]_0[GALDH]_0 K_A} \quad (1b)$$

where $[Cc]_0$ is the stock concentration of Cc, $[GALDH]_0$ is the starting concentration of GALDH in the tube, $\Delta\delta$ is the chemical shift change at a given step in the titration, R is the ratio of the total concentrations of Cc and GALDH, $\Delta\delta_0$ is the change in the chemical shift for 100% bound Cc, and K_A is the association constant. In the fits $\Delta\delta$ and R were the dependent and independent variables, respectively, and $\Delta\delta_0$ and K_A the fitted parameters. The average chemical shift perturbations were derived from the following equation:

$$\Delta\delta_{ave} = \sqrt{\frac{\left(\Delta\delta^{N}/5\right)^2 + \left(\Delta\delta^{H}\right)^2}{2}} \quad (2)$$

where $\Delta\delta^{N}$ and $\Delta\delta^{H}$ are the chemical shift perturbations of the amide nitrogen and proton, respectively. The estimated error in K_A values was ±10%.

Formatted: Justified, Line spacing: 1.5 lines

Acknowledgements

QB was supported by a fellowship from the Higher Education Commission of Pakistan. Research work was supported by a VICI grant from the Netherlands Organisation for Scientific Research to MU (700.58.441), the Spanish Ministry of Science and Innovation (Grant BIO2010-1493) to MM, the Andalusian Government (PAIDI BIO-022), cofinanced with FEDER, to JAN, and the Carbohydrate Research Centre Wageningen (CRC-W) to NGHL. Financial support to IDM was provided by the Spanish Ministry of Economy and Competiveness (Grant No. BFU2009-07190/BMC and BFU2012-31670/BMC) and by the Andalusian Government (Grant PAI, BIO198). BMB was awarded with a PhD fellowship (AP2009-4092) from the Spanish Ministry of Economy and Competitiveness, co-funded by European Social Fund-ERDF (2007-2013). Authors thank the financial support for the form of Access to the Bio-NMR Research Infrastructure co-funded under the 7th Framework Programme of the EC (FP7/ 2007–2013) grant agreement 261863 and project contract RII3–026145.

REFERENCES

1. Joosten V & van Berkel WJH (2007) Flavoenzymes. *Curr Opin Chem Biol* **11**, 195-202.
2. van Berkel WJH (2008) Chemistry of Flavoenzymes. In *Wiley Encyclopedia of Chemical Biology* (Begley T, ed, pp. 1-11. John Wiley & Sons, Inc.
3. Leferink NGH, van den Berg WAM & van Berkel WJH (2008) L-Galactono-γ-lactone dehydrogenase from *Arabidopsis thaliana*, a flavoprotein involved in vitamin C biosynthesis. *FEBS J* **275**, 713-726.
4. Wheeler GL, Jones MA & Smirnoff N (1998) The biosynthetic pathway of vitamin C in higher plants. *Nature* **393**, 365-369.
5. van Hellemond EW, Leferink NGH, Heuts DPHM, Fraaije MW & van Berkel WJH (2006) Occurrence and biocatalytic potential of carbohydrate oxidases. In *Advances in Applied Microbiology* (Laskin AI, Sariaslani S & Gadd GM, eds), pp. 17-54. Academic Press.
6. Schertl P, Sunderhaus S, Klodmann J, Grozeff GE, Bartoli CG & Braun HP (2012) L-galactono-1,4-lactone dehydrogenase (GLDH) forms part of three subcomplexes of mitochondrial complex I in *Arabidopsis thaliana*. *J Biol Chem* **287**, 14412-14419.
7. Tollin G (1995) Use of flavin photochemistry to probe intraprotein and interprotein electron transfer mechanisms. *J Bioenerg Biomembr* **27**, 303-309.
8. Edmondson DE & Tollin G (1983) Semiquinone formation in flavo- and metalloflavoproteins. *Top Curr Chem* **108**, 109-138.
9. Navarro JA, Cheddar G & Tollin G (1989) Laser flash photolysis studies of the kinetics of reduction of spinach and Clostridium ferredoxins by a viologen analogue: Electrostatically controlled nonproductive complex formation and differential reactivity among the iron-sulfur clusters. *Biochemistry* **28**, 6057-6065.
10. Rodríguez-Roldán V, Garcia-Heredia JM, Navarro JA, Hervás M, de la Cerda B, Molina-Heredia FP & de la Rosa MA (2006) A comparative kinetic analysis of the reactivity of plant, horse, and human respiratory cytochrome c towards cytochrome c oxidase. *Biochem Biophys Res Commun* **346**, 1108-1113.
11. Hervás M, Navarro JA, Díaz A, Bottin H & de la Rosa MA (1995) Laser-flash kinetic analysis of the fast electron transfer from plastocyanin and cytochrome c_6 to photosystem I. Experimental evidence on the evolution of the reaction mechanism. *Biochemistry* **34**, 11321-11326.

12. Meyer TE, Zhao ZG, Cusanovich MA & Tollin G (1993) Transient kinetics of electron transfer from a variety of c-type cytochromes to plastocyanin. *Biochemistry* **32**, 4552-4559.

13. Watkins JA, Cusanovich MA, Meyer TE & Tollin G (1994) A "parallel plate" electrostatic model for bimolecular rate constants applied to electron transfer proteins. *Protein Sci* **3**, 2104-2114.

14. Hazzard JT, Rong SY & Tollin G (1991) Ionic strength dependence of the kinetics of electron transfer from bovine mitochondrial cytochrome c to bovine cytochrome c oxidase. *Biochemistry* **30**, 213-222.

15. Volkov AN, Bashir Q, Worrall JAR, Ullmann GM & Ubbink M (2010) Shifting the equilibrium between the encounter state and the specific form of a protein complex by interfacial point mutations. *J Am Chem Soc* **132**, 11487-11495.

16. Volkov AN, Ferrari D, Worrall JAR, Bonvin AMJJ & Ubbink M (2005) The orientations of cytochrome *c* in the highly dynamic complex with cytochrome b_5 visualized by NMR and docking using HADDOCK. *Protein Sci* **14**, 799-811.

17. Worrall JAR, Liu U, Crowley PB, Nocek JM, Hoffman BM & Ubbink M (2002) Myoglobin and cytochrome b_5: a nuclear magnetic resonance study of a highly dynamic protein complex. *Biochemistry* **41**, 11721-11730.

18. Worrall JAR, Reinle W, Bernhardt R & Ubbink M (2003) Transient protein interactions studied by NMR spectroscopy: the case of cytochrome *c* and adrenodoxin. *Biochemistry* **42**, 7068-7076.

19. Leferink NGH, Heuts DPHM, Fraaije MW & van Berkel WJH (2008) The growing VAO flavoprotein family. *Arch Biochem Biophys* **474**, 292-301.

20. Alhagdow M, Mounet F, Gilbert L, Nunes-Nesi A, Garcia V, Just D, Petit J, Beauvoit B, Fernie AR, Rothan C, et al. (2007) Silencing of the mitochondrial ascorbate synthesizing enzyme L-galactono-1,4-lactone dehydrogenase (L-GalLDH) affects plant and fruit development in tomato. *Plant Physiol* **145**, 1408-1422.

21. Bartoli CG, Pastori GM & Foyer CH (2000) Ascorbate biosynthesis in mitochondria is linked to the electron transport chain between complexes III and IV. *Plant Physiol* **123**, 335-344.

22. Leferink NGH, van Duijn E, Barendregt A, Heck AJR & van Berkel WJH (2009) Galactonolactone dehydrogenase requires a redox-sensitive thiol for optimal production of vitamin C. *Plant Physiol* **150**, 596-605.

23. Leferink NGH, Fraaije MW, Joosten HJ, Schaap PJ, Mattevi A & van Berkel WJH (2009) Identification of a gatekeeper residue that prevents dehydrogenases from acting as oxidases. *J Biol Chem* **284**, 4392-4397.

24. Worrall JAR, Kolczak U, Canters GW & Ubbink M (2001) Interaction of yeast iso-1-cytochrome c with cytochrome c peroxidase investigated by [^{15}N,^{1}H] heteronuclear NMR spectroscopy. *Biochemistry* **40**, 7069-7076.

25. Crowley PB, Rabe KS, Worrall JAR, Canters GW & Ubbink M (2002) The ternary complex of cytochrome *f* and cytochrome *c*: identification of a second binding site and competition for plastocyanin binding. *Chembiochem* **3**, 526-533.

26. Ubbink M & Bendall DS (1997) Complex of plastocyanin and cytochrome *c* characterized by NMR chemical shift analysis. *Biochemistry* **36**, 6326-6335.

27. Bashir Q, Scanu S & Ubbink M (2011) Dynamics in electron transfer protein complexes. *FEBS J* **278**, 1391-1400.

28. Morar AS, Kakouras D, Young GB, Boyd J & Pielak GJ (1999) Expression of ^{15}N-labeled eukaryotic cytochrome *c* in *Escherichia coli*. *J Biol Inorg Chem* **4**, 220-222.

29. Pollock WB, Rosell FI, Twitchett MB, Dumont ME & Mauk AG (1998) Bacterial expression of a mitochondrial cytochrome *c*. Trimethylation of lys72 in yeast iso-1-cytochrome c and the alkaline conformational transition. *Biochemistry* **37**, 6124-6131.

30. Margoliash E & Frohwirt N (1959) Spectrum of horse-heart cytochrome *c*. *Biochem J* **71**, 570-572.

31. Moore GR & Pettigrew GW (1990) *Cytochromes c. Evolutionary, structural and physicochemical aspects.* Springer-Verlag, Berlin.

32. Navarro JA, Hervás M, Pueyo JJ, Medina M, Gómez-Moreno C, de la Rosa MA & Tollin G (1994) Laser flash-induced photoreduction of photosynthetic ferredoxins and flavodoxin by 5-deazariboflavin and by a viologen analogue. *Photochem Photobiol* **60**, 231-236.

33. Rodríguez-Roldán V, García-Heredia JM, Navarro JA, Hervás M, de la Cerda B, Molina-Heredia FP & de la Rosa MA (2008) Effect of nitration on the physico-chemical and kinetic features of wild-type and mono-tyrosine mutants of human respiratory cytochrome c. *Biochemistry* **47**, 12371-12379.

34. Pierce MM, Raman CS & Nall BT (1999) Isothermal titration calorimetry of protein-protein interactions. *Methods* **19**, 213-221.

35. Volkov AN, Vanwetswinkel S, van de Water K & van Nuland NAJ (2012) Redox-dependent conformational changes in eukaryotic cytochromes revealed by paramagnetic NMR spectroscopy. *J Biomol NMR* **52**, 245–256.

36. Delaglio F, Grzesiek S, Vuister GW, Zhu G, Pfeifer J & Bax A (1995) NMRPipe: a multidimensional spectral processing system based on UNIX pipes. *J Biomol NMR* **6**, 277-293.

37. Vranken WF, Boucher W, Stevens TJ, Fogh RH, Pajon A, Llinas M, Ulrich EL, Markley JL, Ionides J & Laue ED (2005) The CCPN data model for NMR spectroscopy: development of a software pipeline. *Proteins* **59**, 687-696.

38. Louie GV & Brayer GD (1990) High-resolution refinement of yeast iso-1-cytochrome *c* and comparisons with other eukaryotic cytochromes *c*. *J Mol Biol* **214**, 527-555.

Supporting Information

Figure S1. Clustal W multiple sequence alignment of Cc.

Figure S2. Mechanisms of GALDH oxidation by cytochromes c (Cc).

Legends to figures

Figure 1. Laser-flash kinetic traces of $GALDH_{SQ}$ generation and decay measured at 433 nm in a solution containing 50 µM $GALDH_{OX}$ in 10 mM Tris-HCl buffer, pH 7.5, 2 mM EDTA, 100 µM dRf, 1 mM PDQ, and 0.02% ß-dodecyl-maltoside, in the absence (A, B) or presence (C) of *Arabidopsis* Cc_{OX} 10 µM. Other experimental conditions were as indicated in Experimental Procedures.

Figure 2. (*Upper*) Dependence of k_{obs} for $GALDH_{SQ}$ oxidation on the concentration of either horse or *Arabidopsis* Cc_{OX}. Experiments were carried out as described for Figure 1. Line fittings correspond to the reaction mechanisms previously proposed [12]. (*Lower*) Dependence on the square root of ionic strength of k_{obs} for $GALDH_{SQ}$ oxidation by horse or *Arabidopsis* Cc_{OX} as studied by laser-flash spectroscopy, in solutions containing 50 µM GALDH and 12 µM Cc. Continuous line fittings correspond to the electrostatic interaction model previously proposed [13]. (*Lower Inset*) Dependence of k_{obs} for $GALDH_{SQ}$ (open circles) and $GALDH_{HQ}$ (closed squares) oxidation on the concentration of *Arabidopsis* Cc_{OX} in the presence of 150 mM NaCl followed respectively by laser-flash spectroscopy and stopped-flow. Other experimental conditions were as indicated in Experimental Procedures.

Figure 3. ITC data for the interaction between GALDH and *Arabidopsis* Cc at 25 °C. A $GALDH_{OX}$ solution (120 µM) was titrated with successive 7.5 µL additions of a 3 mM solution of Cc_{OX}. Data fitting to the standard model assuming no-cooperative interaction allows an estimation of the binding stoichiometry, the K_A and the binding enthalpy and entropy values for the interaction process. (*Inset*) Raw data of the titration. Other experimental conditions were as indicated in Experimental Procedures.

Figure 4. Chemical shift perturbations of Cc backbone amides upon binding with GALDH. A, C and E show the chemical shift perturbations of *Arabidopsis* Cc_{RED} in complex with $GALDH_{OX}$. B, D and F represent the chemical shift perturbations of yeast Cc_{OX} in complex with $GALDH_{OX}$. The average perturbations (equation 2) are shown in panels E and F. The values of Δδ are extrapolated to 100% bound Cc.

Figure 5. Surface representation of the Cc residues interacting with GALDH. The residues are colored according to the size of chemical shift changes in ^{15}N dimension ($\Delta\delta^N$), red ($\Delta\delta$ > 0.3 ppm), orange ($\Delta\delta$ > 0.2 ppm), yellow ($\Delta\delta$ > 0.1 ppm) and cyan ($\Delta\delta$ > 0.05 ppm). The blue surface represents unaffected residues ($\Delta\delta$ < 0.05 ppm) and grey surface shows the residues not observed in the HSQC spectrum. A and B represent two sides of *Arabidopsis* Cc_{RED} in complex with $GALDH_{OX}$, C and D represent two sides of yeast Cc_{OX} in complex with $GALDH_{OX}$. The values of $\Delta\delta$ are extrapolated to 100% bound Cc. The figure was made using the crystal structure of yeast Cc (PDB entry 1YCC [38]).

Figure 6. Binding shifts of Cc ^{15}N amide resonances upon binding with $GALDH_{OX}$. A) binding curves for *Arabidopsis* Cc_{RED}; B) binding curve for yeast Cc_{OX}. For *Arabidopsis* Cc_{RED} the titration curves are shown for residues T12, K13, G29 and an unassigned residue. For yeast Cc_{OX} the titration curve is shown for T12. The curves are fitted to a 1:1 binding model (solid lines).

FEBS Journal

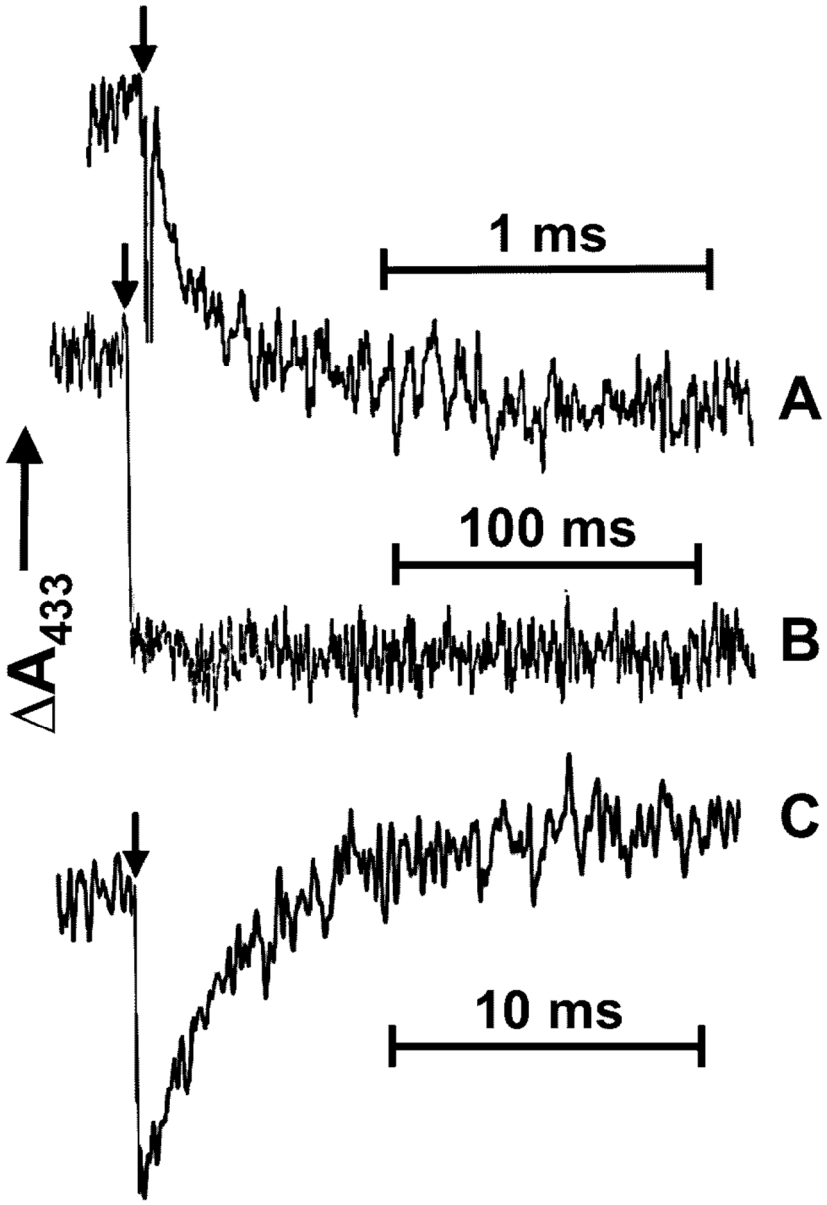

83x120mm (300 x 300 DPI)

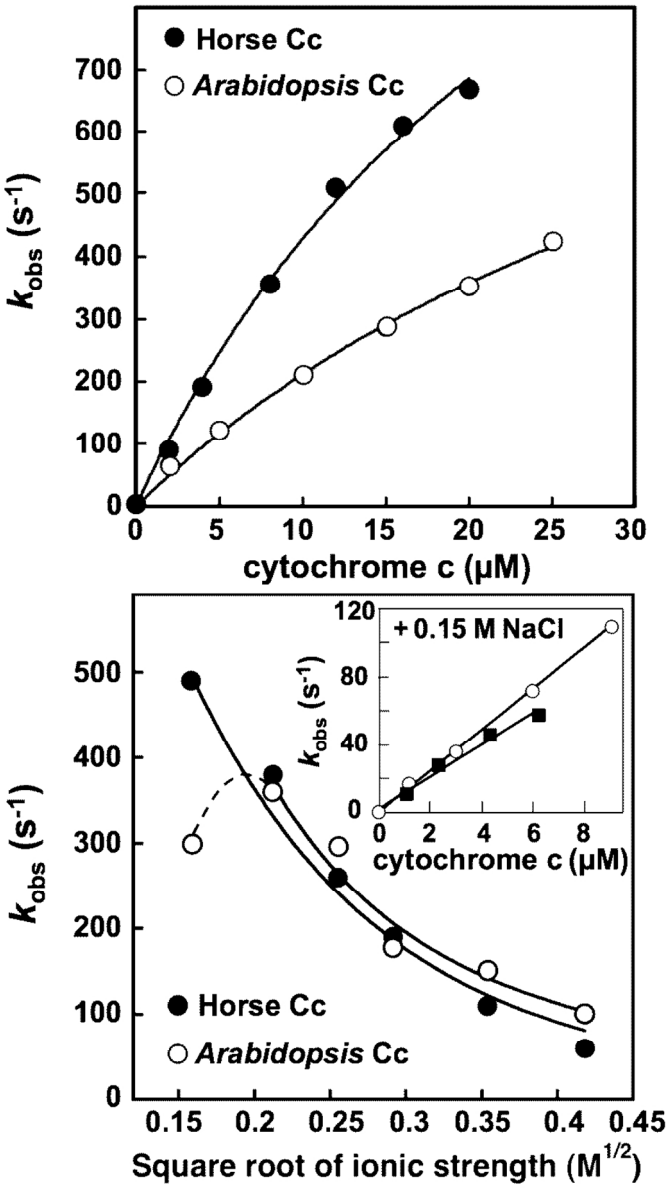

80x140mm (300 x 300 DPI)

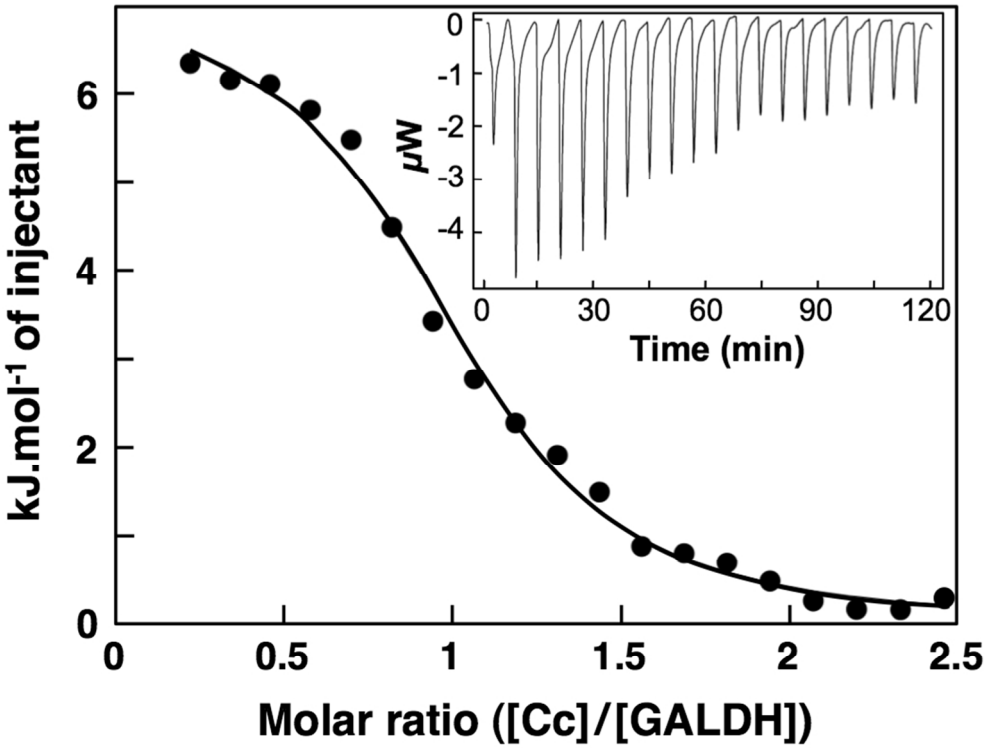

89x68mm (300 x 300 DPI)

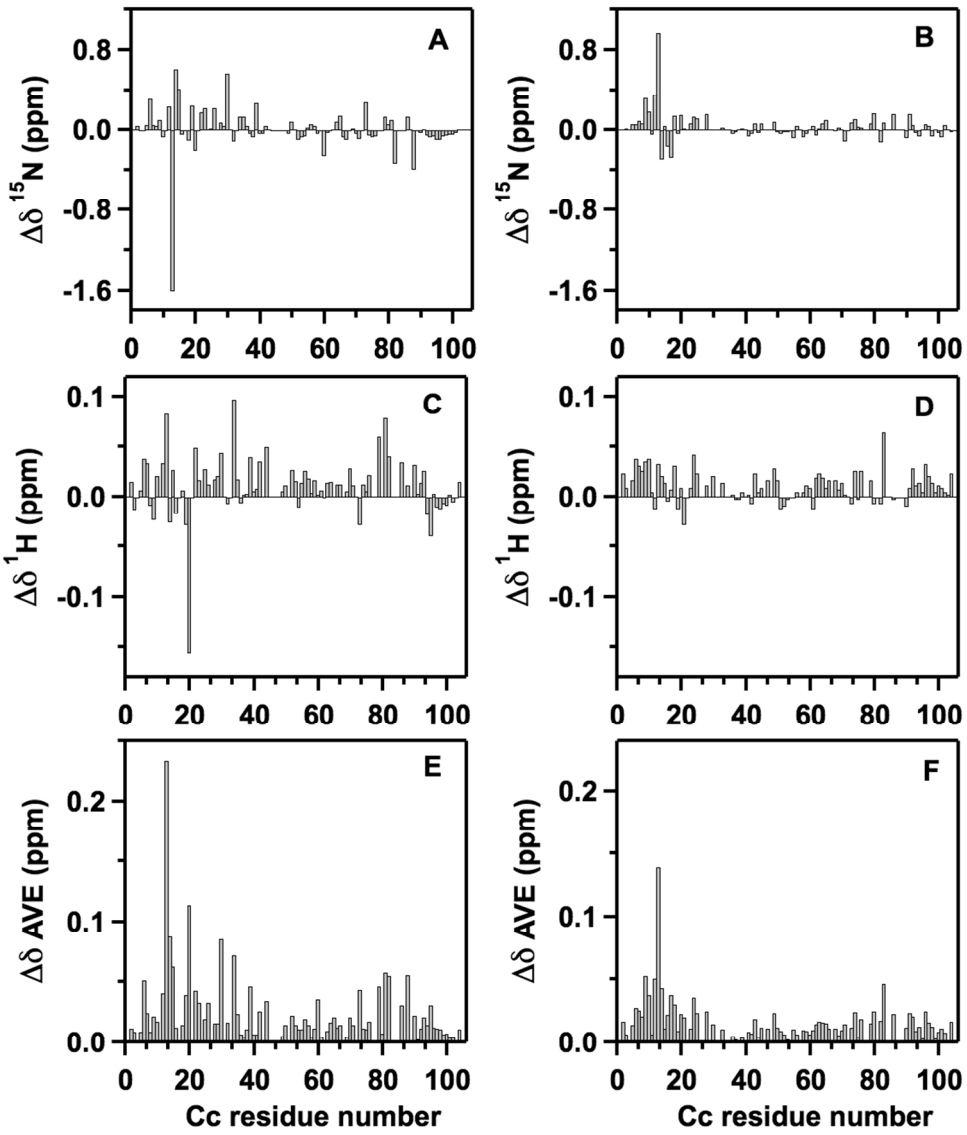

198x228mm (150 x 150 DPI)

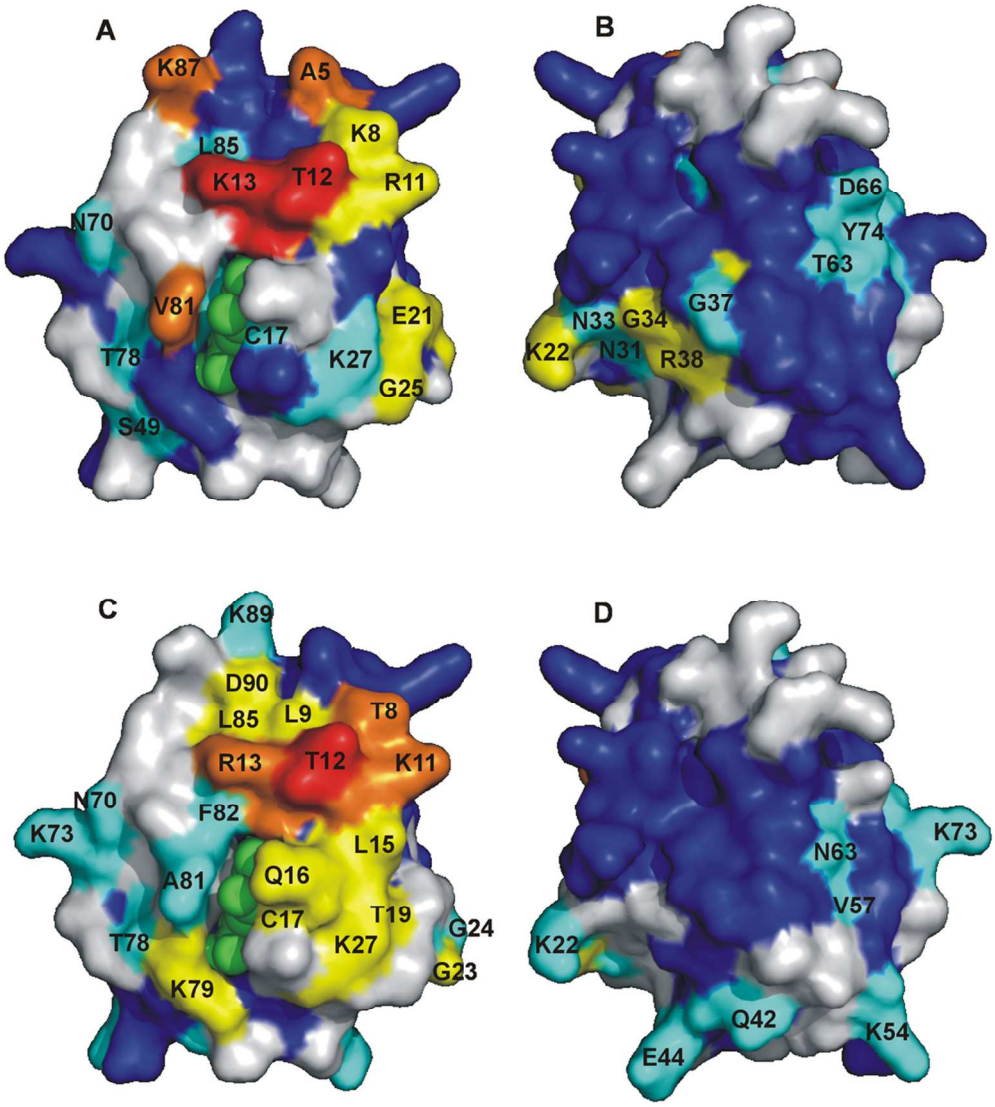

98x109mm (300 x 300 DPI)

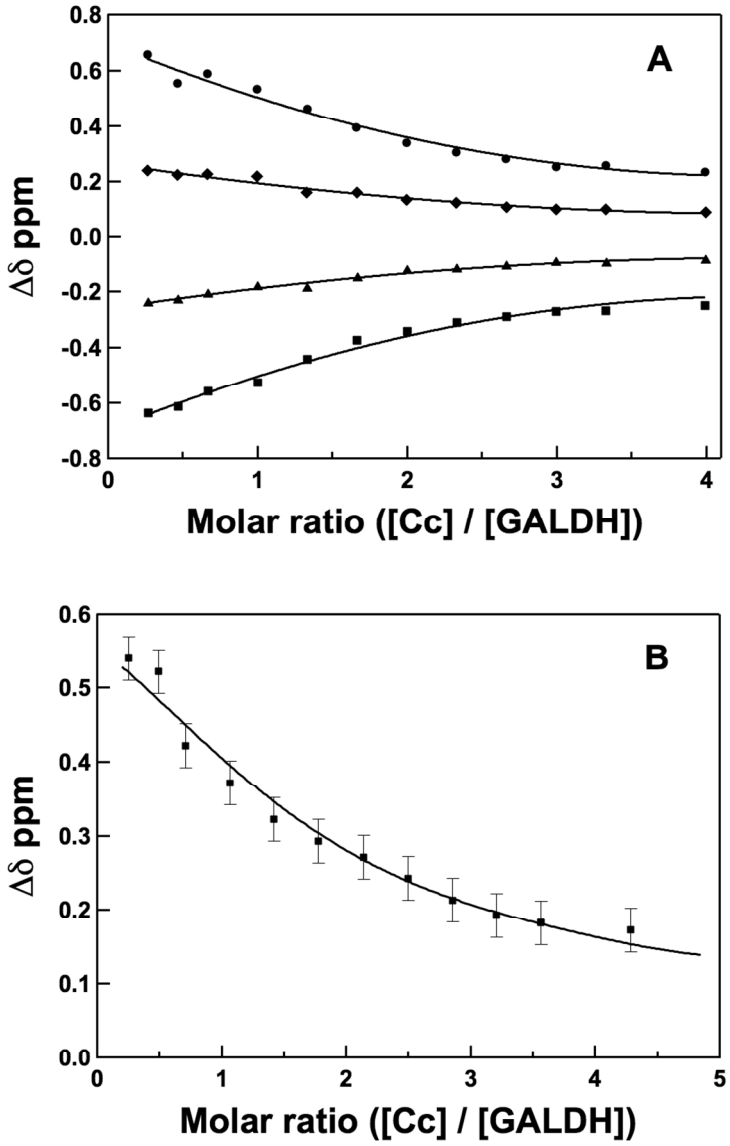

388x579mm (72 x 72 DPI)

50x14mm (300 x 300 DPI)

FEBS Journal

Table 1. Kinetic and thermodynamic parameters for the interaction between GALDH and Cc.

Protein couple	K_D	k_{ET}	[a]k_2	[b]k_{inf}	ΔG	ΔH	-TΔS
	μM	s^{-1}	$M^{-1}\ s^{-1}$	$M^{-1}\ s^{-1}$	kJ mol^{-1}	kJ mol^{-1}	kJ mol^{-1}
[c]$GALDH_{SQ}$/Horse Cc_{OX}	17	1,720	0.6×10^7	0.9×10^6	-27.3		
[c]$GALDH_{SQ}$/*Arabidopsis* Cc_{OX}	31	1,200	1.2×10^7	1.3×10^6	-20.0		
[d]$GALDH_{HQ}$/*Arabidopsis* Cc_{OX}			0.9×10^7				
[e]$GALDH_{OX}$/*Arabidopsis* Cc_{OX}	17				-27.3	7.6	-34.8
[e]$GALDH_{OX}$/*Arabidopsis* Cc_{RED}	13				-27.9	9.0	-36.9
[f]$GALDH_{OX}$/Yeast Cc_{OX}	50				-19.2		
[f]$GALDH_{OX}$/*Arabidopsis* Cc_{RED}	77				-18.1		

[a)]Second-order rate constant obtained from the linear concentration dependences in the presence of 0.15 M NaCl. [b)]Second-order rate constant extrapolated to infinite ionic strength estimated by applying the formalism described in [13]. [c)]Values obtained by laser-flash spectroscopy. [d)]Obtained by stopped-flow kinetics analysis. [e)]Values determined by ITC analysis. [f)]Values determined by NMR binding studies. See text for more detail.

Figure S2

$$GALDH_{RED} + Cc_{OX} \underset{}{\overset{K_A}{\rightleftharpoons}} [GALDH_{RED}\cdots Cc_{OX}] \xrightarrow{k_{ET}} GALDH_{OX} + Cc_{RED}$$

$$GALDH_{RED} + Cc_{OX} \overset{K_A}{\rightleftharpoons} [GALDH_{RED}\cdots Cc_{OX}] \overset{K_R}{\rightleftharpoons} [GALDH_{RED}\cdots Cc_{OX}]^* \xrightarrow{k_{ET}} GALDH_{OX} + Cc_{RED}$$

124x47mm (300 x 300 DPI)